ACS APPLIED MATERIALS & INTERFACES

Research Article

www.acsami.org

Effect of Isomerism and Chain Length on Electronic Structure, Photophysics, and Sensitizer Efficiency in Quadrupolar (Donor)$_2$–Acceptor Systems for Application in Dye-Sensitized Solar Cells

Coralie A. Richard,[†] Zhenxing Pan,[‡] Hsien-Yi Hsu,[‡] Seda Cekli,[‡] Kirk S. Schanze,[‡] and John R. Reynolds*[,†]

[†]School of Chemistry and Biochemistry, School of Materials Science and Engineering, Center for Organic Photonics and Electronics, Georgia Institute of Technology, Atlanta, Georgia 30332-0400, United States

[‡]Department of Chemistry and Center for Macromolecular Science and Engineering, University of Florida, Gainesville, Florida 32611-7200, United States

Supporting Information

ABSTRACT: We report on quadrupolar (donor)$_2$–acceptor sensitizers for dye-sensitized solar cells (DSSCs). The acceptor units are based on dithieno[2,3-a:3′,2′-c]phenazine and dithieno[3,2-a:2′,3′-c]phenazine coupled to thiophene donors. The optoelectronic and photophysical properties of two sets of isomers reveal a rigid structure for linear isomers and an efficient nonradiative decay for branched isomers. These sensitizers were integrated into DSSCs, and the quadrupolar structure is an operational design, as the IPCE reached up to 38% from 400 nm to 600 nm. The lengthening of the donor chain increases the efficiency, demonstrating the appeal of these oligomeric dyes for DSSCs.

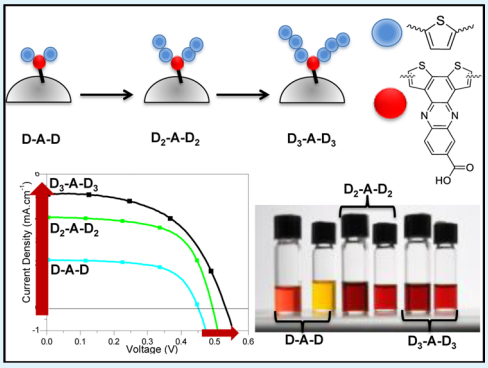

KEYWORDS: *dye-sensitized solar cells, thiophene oligomeric dyes, donor–acceptor interactions, photovoltaic*

INTRODUCTION

Dye-sensitized solar cells (DSSCs) are photovoltaic devices that are highly efficient for solar conversion and operate by interfacing a dye sensitizer with a wide-bandgap metal oxide.[1−3] Dyes originally consisted of transition metal complexes, mainly based on ruthenium.[3] While these sensitizers are efficient, they are expensive to produce and have limited absorption and limited tunability.[4] To resolve these issues, organic dyes have been developed and, upon proper adjustments, have shown equal efficiency compared to inorganic dyes.[4,5] Recently, highly effective perovskite cells proved the usefulness of a hybrid solar cells system, achieving efficiencies from 10.2%[6] to 15%.[7,8]

Most organic dyes tend to be designed with a dipolar D-π-A architecture, where the donor (D) is linked to the metal oxide bound acceptor (A) via a π-conjugated bridge (π).[9,10] To improve device performance, studies largely focus on varying the nature of the sensitizer moieties, with a few others varying the overall design of the sensitizer. For instance, Fisher *et al.*[11] reported on D-π-A dyes where the π-bridge is composed of linear or branched oligothiophene units. They observed that the performance of the isomers differs due to the dye coverage. Moreover, Ning *et al.*[12] reported on starburst shaped dyes, a D-D-π-A structure, and demonstrated that the device performance decreased with the number of donors. Recently, this D-D-π-A type structure with carbazole-based dyes provided cells with a photovoltage over 770 mV and a long term photostability.[13]

In this article, we report a fundamental study of quadrupolar D_2A sensitizers, enabled by the synthesis of a set of isomers employing fused arylenes of internal donor–acceptor (A) nature having metal oxide binding sites appended to the acceptor portion, flanked by two donors (D), each consisting of one to three thiophene units. In this sensitizer design, π-bridge units were not employed, as the donor moieties are directly linked to the acceptor part of the molecule. The external thiophene donors, grafted on different sites of the acceptor, lead to positional isomeric dyes: linear (**L**) where the conjugation is along the donor moieties and branched (**B**) where the conjugation extends all the way through the acceptor. Figure 1 presents the structures of the sensitizers studied. The numbers refer to the total number of thiophene units in the sensitizer.

This is, to our knowledge, the first report of a structure-property relationship for sensitizers with different conjugation pathways. A full electrochemical and photophysical study permits the characterization of the ground and the excited

Received: January 24, 2014
Accepted: March 13, 2014
Published: March 25, 2014

   dx.doi.org/10.1021/am500535k | *ACS Appl. Mater. Interfaces* 2014, 6, 5221−5227

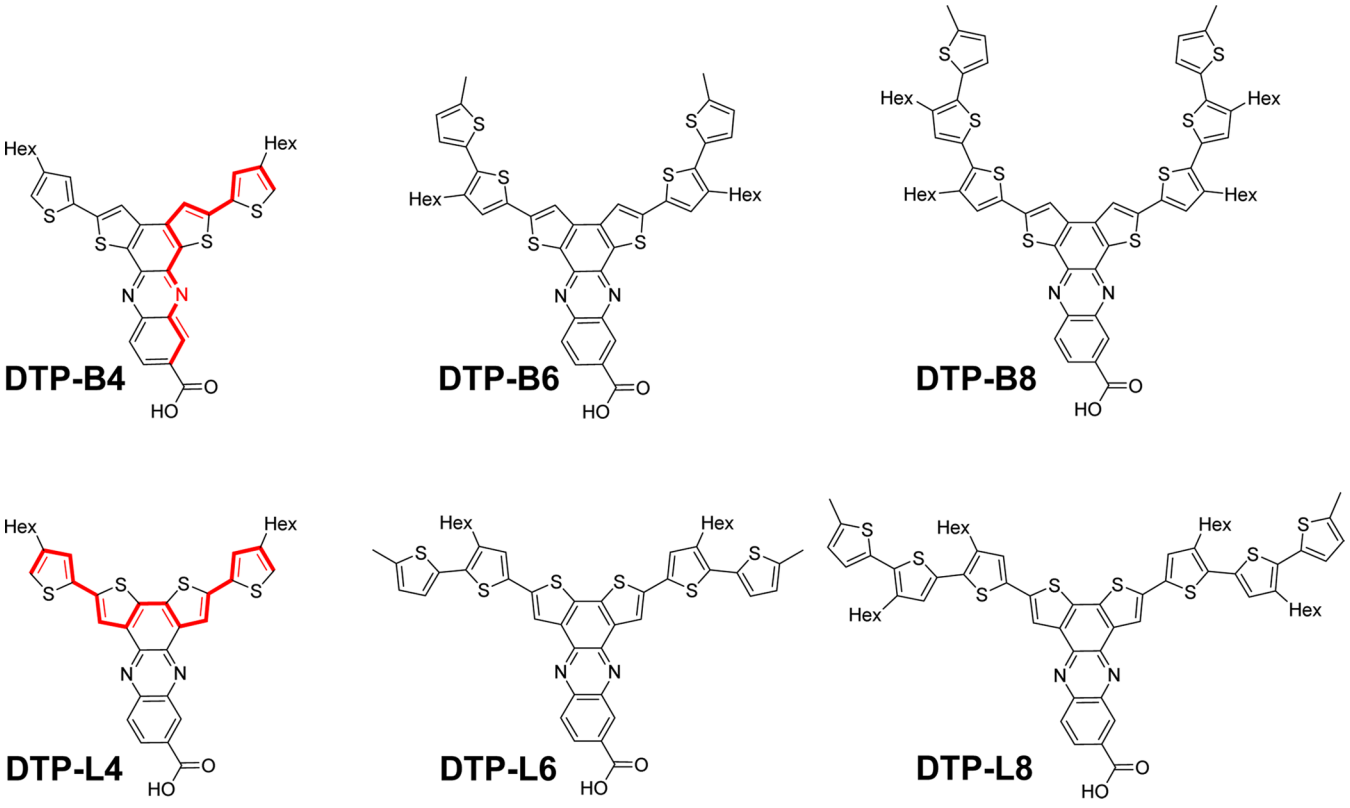

Figure 1. Structures of the sensitizers. The conjugation paths for linear (**DTP-LX** series) and branched (**DTP-BX** series) dyes are shown in red.

states. When used as sensitizers in DSSCs, the quadrupolar structure is successful, and the incident photon to current efficiency (IPCE) reaches 38%. By lengthening the thiophene chain, the light-harvesting capacity of the dyes increases, while the HOMO levels remain suitable for dye regeneration. Consequently, the overall efficiency increases for longer oligomers. Interestingly, the isomers have different radiative and nonradiative decay rates but similar photovoltaic results.

EXPERIMENTAL SECTION

General Procedures. All starting materials and reagents were purchased from known commercial sources and used without further purification, unless otherwise noted. ^{1}H and ^{13}C NMR spectra were collected on a Mercury 300 or a Bruker 400. Chemical shifts were referenced to the residual solvent peaks. High-resolution mass spectrometry was performed by the spectroscopic services in the Chemistry Department of the Georgia Institute of Technology. FTIR measurements were carried out on a Perkin-Elmer Spectrum One FTIR outfitted with a $LiTaO_3$ detector.

Calculations. Geometry optimizations were carried out in the gas phase using the B3LYP [The citation can be found in the Supporting Information.] hybrid functional and the 6-31G* basis set. Frequency calculations were used to characterize the stationary point obtained. All calculations were performed using the Gaussian09 program package [The citation can be found in the Supporting Information.], and the orbitals were represented using the Chemcraft 1.6 program using 0.03 e/bohr^3 as the isodensity value.

Electrochemistry. Cyclic voltammetry and differential pulse voltammetry were performed using an EG&G Princeton Applied Research model 273A potentiostat-galvanostat in an argon filled drybox. The solutions were made from 0.1 M tetrabutylammonium hexafluorophosphate ($TBAPF_6$) in freeze-pump-thawed dichloromethane as the supporting electrolyte. The working electrode was a platinum button, the counter electrode was a platinum flag, and the reference electrode was a $Ag/AgNO_3$ electrode. Scans were calibrated against the ferrocene/ferrocenium (Fc/Fc^+) redox couple (5.12 eV vs vacuum).[14]

Photophysics. UV-vis spectra were recorded on a Cary 5000 (Varian) spectrophotometer. Steady state emission spectra were recorded on a spectrofluorimeter from Photon Technology International and corrected using correction factors generated with a primary standard lamp. Fluorescence lifetimes were determined on a Picoquant FluoTime 100 time-correlated single photon counting instrument. The concentrations of solutions were adjusted to approximately 0.2 absorbance at 375 nm based on the quantum yields of DTP-L and DTP-B series. Nanosecond transient absorption measurements were conducted on a home-built apparatus. The excitation wavelength was generated by a Continuum Surelite OPO Plus pumped with the third harmonic (355 nm) of a Continuum Surelite II-10 Nd:YAG laser. A Xenon arc lamp was used as a probe source. A Triax 180 monochromator and a Si amplified photodetector from Thorlabs (PDA8A) were used for detection at single wavelength.

Dye-Sensitized Solar Cells. The nanocrystalline titanium dioxide (TiO_2) electrode and the platinum cathode were prepared according to the literature.[15] Two holes (1 mm diam.) were drilled into the FTO/platinum glass cathodes for later electrolyte solution injection. A solution of 0.2 mM of dye in DMF was stirred overnight, and the TiO_2 electrodes were immersed in the solution for 36 h. After rinsing with DMF and acetone to remove the unbound dye, the electrodes were placed under vacuum for 2 h for further drying. The dried anodes and platinum cathodes were sealed together with surlyn (Solaronix Meltonix 1170-25). An electrolyte solution containing 0.05 M I_2, 0.1 M LiI, 0.6 M 1-methyl-3-(n-propyl)imidazolium iodide, and 0.5 M 4-tert-butylpyridine in butyronitrile was injected into the sealed device. For incident photon to current efficiency (IPCE) characterization, an Oriel Apex monochromator illuminator coupled with a 1/4m Oriel Cornerstone spectrometer was used to illuminate the cell with monochromatic light. The photocurrent response was recorded under short circuit conditions at 10 nm intervals using a Keithley 2400 source meter under an AM1.5 (100 mW/cm^2) solar simulator. The light intensity at each wavelength was calibrated with an energy meter (S350, UDT Instruments). APCE was calculated following with the

equation: $APCE = (IPCE)/(1 - 10^{-A})$ with A being the absorbance of the films.[9]

RESULTS AND DISCUSSION

Computational Considerations. All molecules were modeled using DFT computations, at the B3LYP/6-31G* level in vacuum. Independent of the isomer or chain length, the LUMO is localized on the acceptor. The proximity of the LUMO to the TiO_2 conduction band (CB) should facilitate electron transfer from the excited state to the TiO_2 CB. By contrast, the HOMO localization is dependent on the structural isomer. For the **L** family, the HOMOs are localized on the thiophene segments (Figure 2 and S1). However, for **DTP-B4** and **DTP-B6** (Figure S1), the HOMOs are localized within the donor segment and spread into the acceptor. In **DTP-B8**, the HOMO and HOMO-1, mainly centered on the donors segments, are nearly degenerate (Figure S2). Time-dependent density functional theory (TDDFT) calculations provided the simulated absorption spectra as well as the associated transitions (Figure S3). For both families, a red shift is predicted with the lengthening of the donor unit, as increasing the number of thiophenes in the donor unit extends the conjugation and reduces the energy gap. The HOMO appears to be more delocalized in the **L** family, and the absorption is red shifted compared to the **B** family. When examining the vertical transitions associated with the first excited state, the **L** series has a single vertical transition, mainly composed of HOMO→LUMO character (Table S1, rows 1, 2, and 3). For the **B** series, the first excited states are composed of two transitions (Table S1, rows 4, 5, and 6), that are a combination of HOMO→LUMO and HOMO-1→LUMO.

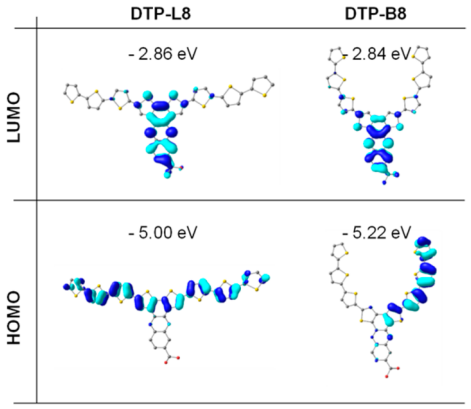

Figure 2. Illustration of frontier molecular orbitals for **DTP-L8** and **DTP-B8** obtained at the B3LYP/6-31G* level in vacuum.

Synthesis. The external donor chains **6** and **8** were built first by consecutive stannylation and Stille coupling from 2-methylthiophene, in good yields (42%–95%), as shown in Scheme 1.

Scheme 2 portrays the synthesis of the acceptor cores via condensation between ethyl 3,4-diaminobenzoate **10** and the corresponding dibromobenzodithiophene-4,5-dione **9** or **12**.[16,17] The reactions were carried out in 10 min in a microwave reactor, in near quantitative yields.

Scheme 2. Synthesis of the Acceptor Cores

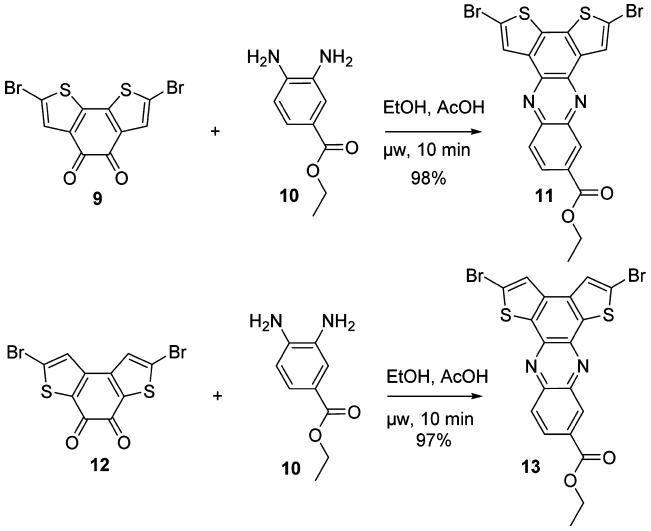

The target molecules were achieved by Stille coupling between the core and the donor blocks. Repeated column chromatography was performed to ensure high purity of the targets, hence lowering the yields to the 20–60% range, as depicted in Scheme 3 for the DTP-L family, and in the Supporting Information (Scheme S1) for the DTP-B family. Finally, quantitative hydrolyses of the ethyl ester derivatives were performed in basic solution. Due to solubility considerations, ester derivatives were used for optical and electrochemical characterizations, and the carboxylic acids derivatives were used in the DSSC devices.

Scheme 1. Synthesis of the External Donor Units[a]

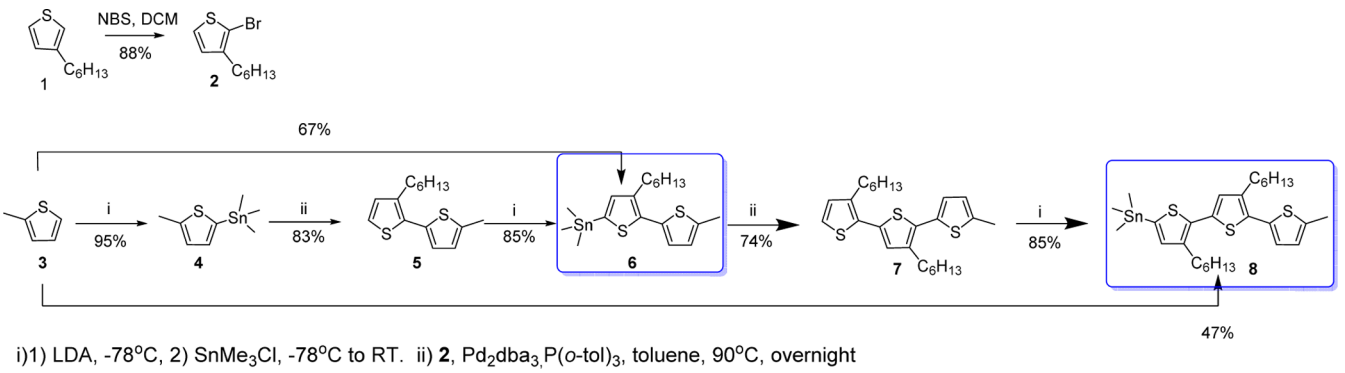

[a]4: one thiophene unit, 6: two thiophenes units, 8: three thiophene units.

Scheme 3. Synthesis of Dyes DTP-L4, DTP-L6, and DTP-L8 and Their Carboxylic Acid Derivatives DTP-L4a, DTP-L6a, and DTP-L8a

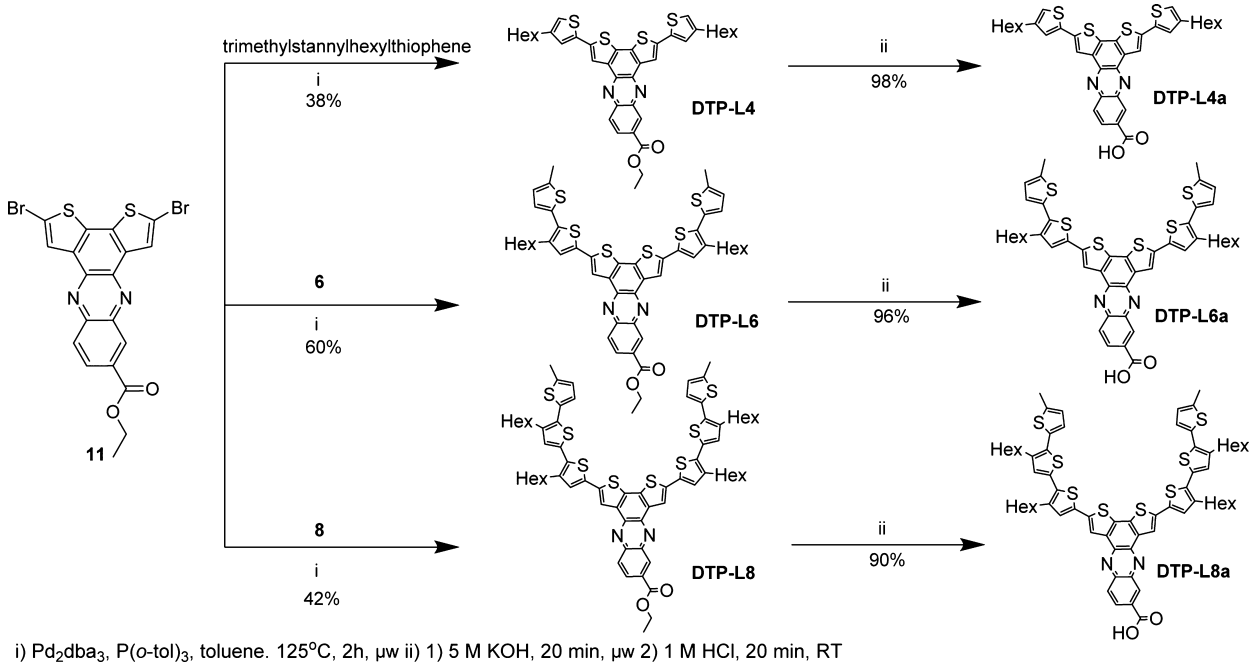

Electrochemical Properties. To probe the frontier orbital energy levels, we used both cyclic voltammetry and differential pulse voltammetry in DCM solutions (Figures S4 and S5). For **DTP-L4** and **DTP-B4,** the oxidation processes were irreversible, as the production of the cation radical leads to dimerization or oligomerization processes.[18] Thus for those compounds, we approximated the HOMO via the difference between the LUMO, obtained by electrochemistry and the lowest energy of optical transition, obtained by spectroscopy. All other sensitizers, end-capped with methyl groups, exhibit reversible oxidations and therefore permit a direct measure of the frontier orbital levels. Quantitatively, the reduction potential for the **L** (Figure S4) series is centered at −1.47 V and at −1.39 V for the **B** series (Figure S5). The oxidative peak potentials decrease with the increase of thiophene donors, in agreement with the DFT calculations. Consequently, the energy gaps decrease with the lengthening of the conjugated system. Frontier orbital levels are gathered in Figure 3 and reflect the fact that all dyes are suitable for electron injection onto the CB of TiO_2 and dye regeneration with the iodide/triiodide redox couple.[19]

Optical Properties. The UV-visible absorption spectra in solution, presented in Figure 4, are consistent with the trends given by DFT calculations and show the red shift of the **L** family. All spectra show strong bands at 300−450 nm and 490−600 nm. Higher energy bands are attributed to local $\pi-\pi^*$ transitions, and lower energy bands correspond to charge transfer (CT) transitions. Broadened and bathochromic shifted spectra are observed in both families with the lengthening of the conjugated chain. However, the red shift is not linear, and the difference in λ_{max} between **DTP-L6** and **DTP-L8** is small, indicating that the effective conjugation length is reached quickly for **DTP-L**. Moreover, the spectra exhibit well resolved fine structure, persisting with the lengthening of the donor chain. This is indicative of a rigidification of the conjugated system.[18] Contrastingly, the effective conjugation length is not reached for the **B** series, and the broad and structureless band

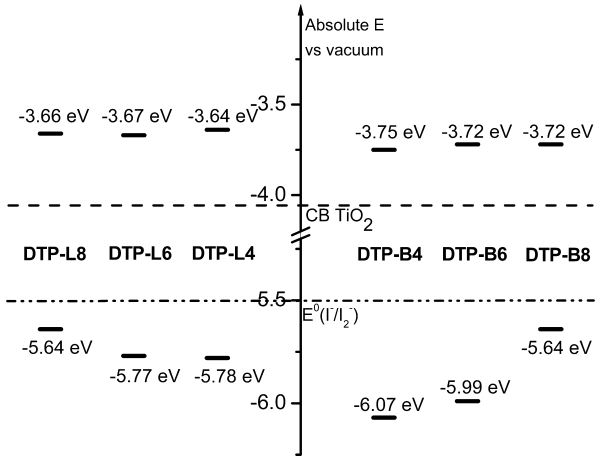

Figure 3. Frontier orbitals of the studied sensitizers obtained by voltammetry.

reflects the multiple transitions forming the vertical transitions (as discussed in the computational section) and the presence of some conformational disorder in the conjugated backbone. Extinction coefficients are high in the $\pi-\pi^*$ region, above 50 000 $M^{-1}\cdot cm^{-1}$ for the **L** family, and above 75 000 $M^{-1}\cdot cm^{-1}$ for the **B** series, which make these molecules attractive as sensitizers.

In order to probe the properties of the singlet excited states for the oligomers, fluorescence studies were carried out in dichloromethane solution, and the results are presented in Table 1. The fluorescence spectra of all oligomers appear as broad, structureless bands (Figure S6). The band maxima for the **DTB-B** series red-shift with increasing oligomer length; however, the fluorescence maximum is similar for **DTP-L6** and **DTP-L8** suggesting that, in this series, the conjugation length is limited to ca. 6 thiophene repeats. (A similar trend is seen in the absorption spectra for the **DTP-L** series.) The fluorescence

dx.doi.org/10.1021/am500535k | ACS Appl. Mater. Interfaces 2014, 6, 5221−5227

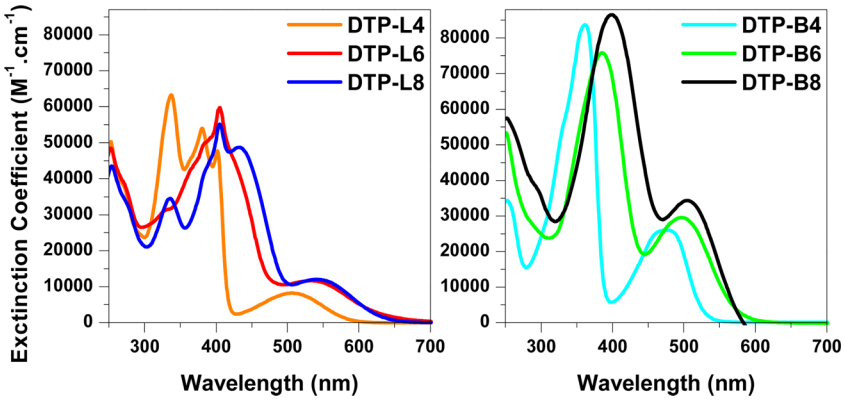

Figure 4. UV-visible spectra of the **DTP-B** and **DTP-L** series in DCM solution.

Table 1. Photophysical Data for DTP-L and DTP-B Series[a]

compd	λ_{max} (nm)[a]	λ_F (nm)[a]	τ_F[b] (ns)	Φ_F[c] (%)	k_r[d] (10^6 s^{-1})	k_{nr}[d] (10^7 s^{-1})
DTP-L4	336, 380, 402, 505	680	10.6	7.4	7.0	8.7
DTP-L6	404, 529	760	3.26	4.7	14.4	29.2
DTP-L8	332, 405, 433, 534	750	1.98	3.5	17.7	48.7
DTP-B4	361, 478	580	0.78	1.3	16.7	126.5
DTP-B6	385, 497	725	0.78	0.8	10.3	127.2
DTP-B8	400, 503	775	0.78	0.5	6.4	127.6

[a]Measurements for DCM solutions at ambient temperature. [b]Emission lifetime measured at fluorescence emission maximum (see left adjacent column). [c]Measured using $Ru(bpy)_3$ (Φ_F = 0.055 in water) as the actinometer. [d]$k_r = \Phi_F/\tau_F$; $k_{nr} = (1 - \Phi_F)/\tau_F$.

quantum yields for the oligomers are comparatively low (Φ_F < 0.07), and they generally decrease with increasing oligomer length. More insight into the excited state dynamics is provided by the fluorescence lifetimes and the radiative and nonradiative rates, which are shown in Table 1. For both series, the radiative rates are in the range of 10^7 s^{-1}, which is on the low-side for conjugated organic chromophores; the reason for this is likely due to the charge transfer character of the lowest singlet states. For the **DTP-L** set, the lifetimes systematically decrease with increasing oligomer length (Figure 5). This decrease is due to a

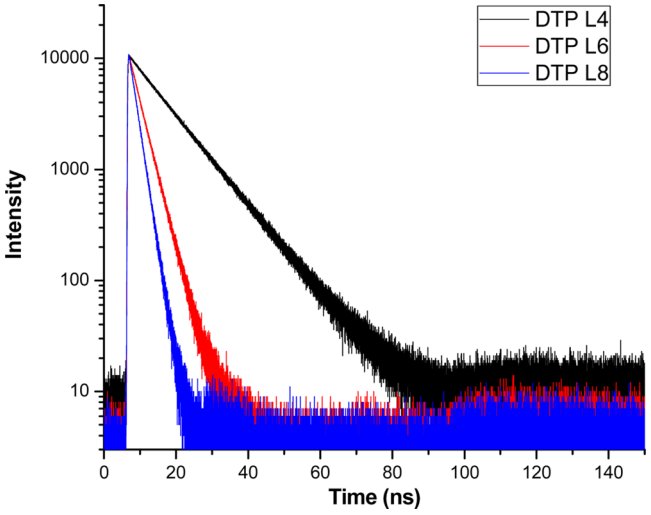

Figure 5. Time-resolved fluorescence spectroscopy of **DTP-L** series.

combined increase in both the radiative and nonradiative decay rate along the series. The increase in k_r is likely due to the increased conjugation, and that for k_{nr} may be due to the charge transfer nature of the singlet excited state.

By contrast, as seen in Figure S7, the lifetimes for all of the **DTP-B** oligomers are comparatively short, and this is due to a relatively constant and large nonradiative decay rate (≈10^9 s^{-1}) for all members of the set. The relatively large nonradiative rates for the oligomers here may also be due to the charge transfer character of the singlet excited state.

Device Characterization. Carboxylic acids derivatives of the oligomers were used for adsorption onto mesoscopic TiO_2 films. Figure S8 shows the UV-visible absorption spectra of the sensitizers adsorbed onto the metal oxide films. All films give rise to relatively strong absorption, with those for the longer oligomers exhibiting >90% absorption (A > 1.0) for λ < 600 nm. Note that the absorption bands are broadened due to the adsorption onto TiO_2.[20,21]

To explore the charge injection and recombination properties of the dyes on TiO_2, nanosecond transient absorption studies were carried out on the TiO_2 film, while they are immersed in degassed ACN solution with $LiClO_4$ electrolyte, as shown in Figure S9. In each case, reasonably strong transient absorption is observed with the signals clearly arising from the oxidized dyes. The spectra for the longer members of the series are obscured at shorter wavelengths, e.g. < 600 nm, due to the strong ground state absorption of the films. Charge recombination kinetic data were satisfactorily fitted exponentially which indicates that charge recombination dynamics is homogeneous and dominated by interfacial electron-transfers.[22] The lifetimes were found to be 502, 65, and 10 μs for **DTPB-4**, **DTPB-6**, and **DTPB-8**, respectively, and 134, 30, and 32 μs for **DTPL-4**, **DTPL-6**, and **DTPL-8**, respectively. The appearance of the strong transient absorption and the relatively long lifetimes (slow recombination) suggest that the dyes should function well as sensitizers in a DSSC configuration.

The dyes were then tested in a standard DSSC set-up as a means of carrying out an initial structure-property relationship comparison. We tested only a single DSSC configuration (e.g., solvent, electrolyte, and additives), so these device results should be viewed as "unoptimized"; therefore, they do not show the maximum efficiencies that can be attained. In this study, the results were reproducible, and all dyes were found to be able to transform photons into charge carriers, as shown in Figure 6. The incident photon to current (IPCE) response plateaued above 38% from 400 nm to 490 nm for **DTP-L8** and above 33% from 420 nm to 540 nm for **DTP-B8**, following the

dx.doi.org/10.1021/am500535k | ACS Appl. Mater. Interfaces 2014, 6, 5221−5227

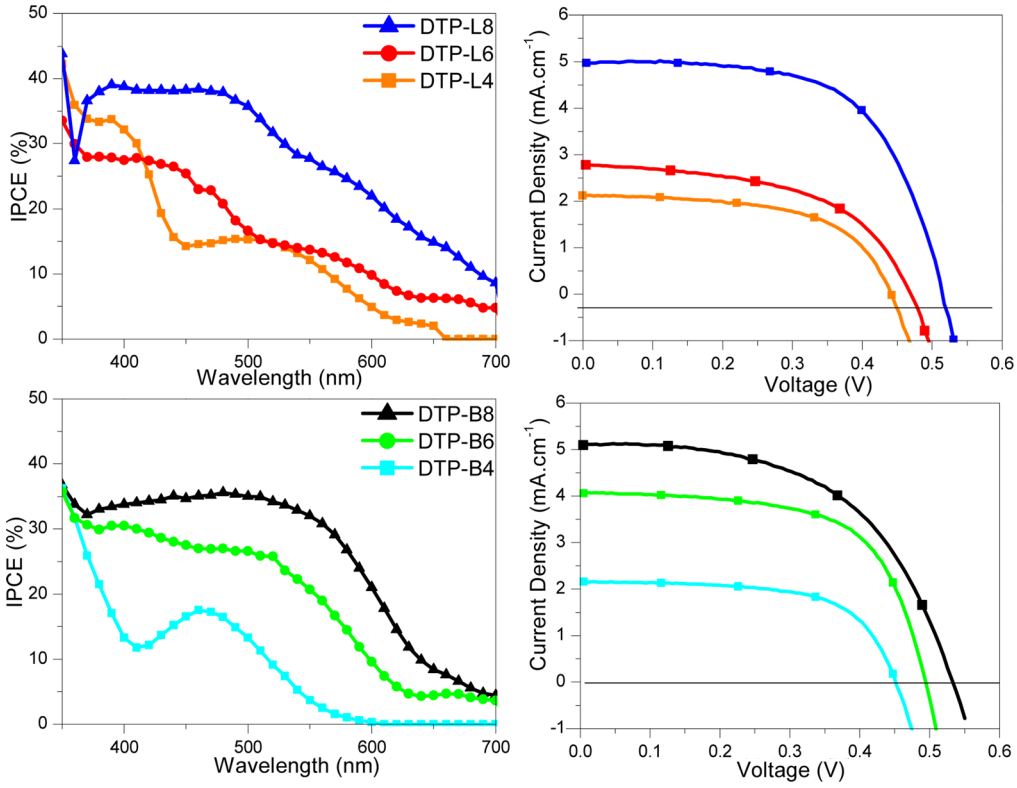

Figure 6. IPCE (left) and J-V (right) measured for DTP-L series (top) and DTP-B series (bottom).

trends observed in the UV-visible absorption spectra of the films. Moreover, the IPCE response extends into the near IR region for **DTP-L6,8** and **DTP-B6,8** (λ > 700 nm). The estimated currents obtained from the IPCE spectra are in good agreement with the measured photocurrent density and range from 2 mA·cm^{-2} for **DTP-L4** and **DTP-B4** to 6 mA·cm^{-2} for **DTP-B8** (Table S2). The absorbed photon to current efficiency (APCE) for the dyes are similar to those obtained for IPCE (Figure S10) and highlight that the electron injection or the electron collection are the intrinsic limiting parameters.[10] As seen in Figure 6, both V_{oc} and J_{sc} increase with the number of thiophene units. For the current density, this is likely due to the absorption of more photons, as demonstrated with UV-visible absorption and IPCE data. The open circuit voltages range from 440 mV for shorter oligomers to 520 mV for longer oligomers, as seen in Table S2. We infer that the long oligothiophene chain impart dye aggregation and recombination between TiO_2 and the redox couple, hence raising the free electron density.[23,24] Interestingly, the V_{oc} are quasi-independent of the isomer used, indicating that the isomer has a relatively minor effect on the surface charge of TiO_2, or on the balance between electron injection and electron recombination. However, the current densities slightly increase for the branched quadrupolar dyes, and that can be related to the dye harvesting properties that are stronger for the **DTP-B** series.

CONCLUSION

In conclusion, we present a new class of isomeric quadrupolar D_2A molecules designed as sensitizers for DSSCs which provide two channels for absorbing light and funneling the energy to a single acceptor attached to TiO_2. The D_2A molecule optical absorptions were red shifted by adding thiophenes units. The linear isomers present a structure more rigid than the branched isomers, reflecting on the relaxation process of the excited states, with the increase of both radiative and nonradiative rates with the lengthening of the donor chain. These molecules were integrated into DSSCs and generate working devices, with a moderate APCE and IPCE. Addition of external donors to the system significantly improves the photovoltaic results, and the increasing trend is linear with the number of donor units added. Interestingly, the isomerism affects slightly the photovoltaics properties even though their solution optoelectronic properties differ. This highlights that the correlation between the properties of dyes in solution and when adsorbed onto TiO_2 films is not straightforward. The difference in the film lifetimes does not affect the electron injection from the sensitizer to the CB of TiO_2 which happens in the time scale of femtoseconds.[9] However, the stronger absorption properties of the branched series permit an increase both in IPCE and J-V.

ASSOCIATED CONTENT

Supporting Information

Synthetic details and structural characterization of all novel compounds, DFT and TDDFT calculations, fluorescence spectra, electrochemistry data, UV-vis spectra, transient absorption spectra, and APCE spectra. This material is available free of charge via the Internet at http://pubs.acs.org.

AUTHOR INFORMATION

Corresponding Author

*E-mail: reynolds@chemistry.gatech.edu.

Author Contributions

The manuscript was written through contributions of all authors. All authors have given approval to the final version of the manuscript.

Notes

The authors declare no competing financial interest.

■ ACKNOWLEDGMENTS

The authors gratefully acknowledge financial support from the Department of Energy (Grant number DE-FG-02-96ER14617). C.A.R. would like to thank Dr. Dan Patel and Dr. Chad Risko for their helpful scientific discussions

■ REFERENCES

(1) O'Regan, B. C.; Grätzel, M. A Low-Cost, High-Efficiency Solar Cell Based on Dye-Sensitized Colloidal TiO_2 Films. *Nature* **1991**, *353*, 737−740.

(2) Hardin, B. E.; Hoke, E. T.; Armstrong, P. B.; Yum, J.; Comte, P.; Tomas, T.; Fréchet, J. M. J.; McGehee, M. D.; Nazeeruddin, K.; Grätzel, M. Increased Light Harvesting in Dye-Sensitized Solar Cells with Energy Relay Dyes. *Nat. Photon.* **2009**, *3*, 406−411.

(3) Gao, F.; Wang, Y.; Shi, D.; Zhang, J.; Wang, M.; Jing, X.; Humphry-Baker, R.; Wang, P.; Zakeeruddin, S. M. Enhance the Optical Absorptivity of Nanocrystalline TiO_2 Film with High Molar Extinction Coefficient Ruthenium Sensitizers for High Performance Dye-Sensitized Solar Cells. *J. Am. Chem. Soc.* **2008**, 10720−10728.

(4) Ooyama, Y.; Harima, Y. Photophysical and Electrochemical Properties, and Molecular Structures of Organic Dyes for Dye-Sensitized Solar Cells. *Chem. Phys. Chem.* **2012**, *13*, 4032−4080.

(5) Zeng, W.; Cao, Y.; Bai, Y.; Wang, Y.; Shi, Y.; Zhang, M.; Wang, F.; Pan, C.; Wang, P. Efficient Dye-Sensitized Solar Cells with an Organic Photosensitizer Featuring Orderly Conjugated Ethylenedioxythiophene and Dithienosilole Blocks. *Chem. Mater.* **2010**, *22*, 1915−1925.

(6) Chung, I.; Lee, B.; He, J.; Chang, R. P. H.; Kanatzidis, M. G. All-Solid-State Dye-Sensitized Solar Cells with High Efficiency. *Nature* **2012**, *485*, 486−490.

(7) Ball, J. M.; Lee, M. M.; Hey, A.; Snaith, H. J. Low-Temperature Processed Meso-Superstructured to Thin-Film Perovskite Solar Cells. *Energy Environ. Sci.* **2013**, *6*, 1739−1743.

(8) Burschka, J.; Pellet, N.; Moon, S.-J.; Humphry-Baker, R.; Gao, P.; Nazeeruddin, M. K.; Grätzel, M. Sequential Deposition as a Route to High-Performance Perovskite-Sensitized Solar Cells. *Nature* **2013**, *499*, 316−320.

(9) Hagfeldt, A.; Boschloo, G.; Sun, L.; Kloo, L.; Pettersson, H. Dye-Sensitized Solar Cells. *Chem. Rev.* **2010**, *110*, 6595−6663.

(10) Liang, M.; Chen, J. Arylamine Organic Dyes for Dye-Sensitized Solar Cells. *Chem. Soc. Rev.* **2013**, *42*, 3453−3488.

(11) Fischer, M. K. R.; Wenger, S.; Wang, M.; Mishra, A.; Zakeeruddin, S. M.; Grätzel, M.; Bäuerle, P. D-π-A Sensitizers for Dye-Sensitized Solar Cells: Linear Vs Branched Oligothiophenes. *Chem. Mater.* **2010**, *22*, 1836−1845.

(12) Ning, Z.; Zhang, Q.; Wu, W.; Pei, H.; Liu, B.; Tian, H. Starburst Triarylamine Based Dyes for Efficient Dye-Sensitized Solar Cells. *J. Org. Chem.* **2008**, *73*, 3791−3797.

(13) Liu, B.; Wang, B.; Wang, R.; Gao, L.; Huo, S.; Liu, Q.; Li, X.; Zhu, W. Influence of Conjugated π-Linker in D−D−π−A Indoline Dyes: Towards Long-Term Stable and Efficient Dye-Sensitized Solar Cells with High Photovoltage. *J. Mater. Chem. A* **2014**, *2*, 804−812.

(14) Thompson, B. C. Variable Band Gap Poly(3,4-Alkylenedioxythiophene)-Based Polymers for Photovoltaic and Electrochromic Applications, University of Florida, 2005.

(15) Fang, Z.; Eshbaugh, A. A.; Schanze, K. S. Low-Bandgap Donor-Acceptor Conjugated Polymer Sensitizers for Dye-Sensitized Solar Cells. *J. Am. Chem. Soc.* **2011**, *133*, 3063−3069.

(16) Arroyave, F. A.; Richard, C. A.; Reynolds, J. R. Efficient Synthesis of Benzo[1,2-b:6,5-b′]dithiophene-4,5-Dione (BDTD) and Its Chemical Transformations into Precursors for π - Conjugated Materials. *Org. Lett.* **2012**, *14*, 6138−6141.

(17) Brookins, R. N.; Berda, E.; Reynolds, J. R. Interchain Interactions in Poly(benzo[1,2-b:4,3-b′]dithiophene)s and the Effect of Substituents on Aggregation. *J. Mater. Chem.* **2009**, *19*, 4197−4204.

(18) Turbiez, M.; Frère, P.; Roncali, J. Stable and Soluble Oligo (3 ,4-Ethylenedioxythiophene) s End-Capped with Alkyl Chains. *J. Org. Chem.* **2003**, *68*, 5357−5360.

(19) Snaith, H. J. Estimating the Maximum Attainable Efficiency in Dye-Sensitized Solar Cells. *Adv. Funct. Mater.* **2010**, *20*, 13−19.

(20) Nazeeruddin, K.; Humphry-Baker, R.; Liska, P.; Grätzel, M. Investigation of Sensitizer Adsorption and the Influence of Protons on Current and Voltage of a Dye-Sensitized Nanocrystalline TiO_2 Solar Cell. *J. Phys. Chem. B* **2003**, *107*, 8981−8987.

(21) Liang, M.; Xu, W.; Cai, F.; Chen, P.; Peng, B.; Chen, J.; Li, Z. New Triphenylamine-Based Organic Dyes for Efficient Dye-Sensitized Solar Cells. *J. Phys. Chem. C* **2007**, *111*, 4465−4472.

(22) Haque, S. A.; Handa, S.; Peter, K.; Palomares, E.; Thelakkat, M.; Durrant, J. R. Supermolecular Control of Charge Transfer in Dye-Sensitized Nanocrystalline TiO_2 Films: Towards a Quantitative Structure-Function Relationship. *Angew. Chem., Int. Ed.* **2005**, *44*, 5740−5744.

(23) Thomas, K. R. J.; Hsu, Y.-C.; Lin, J. T.; Lee, K.-M.; Ho, K.-C.; Lai, C.; Cheng, Y.; Chou, P.-T. 2,3-Disubstituted Thiophene-Based Organic Dyes for Solar Cells. *Chem. Mater.* **2008**, *20*, 1830−1840.

(24) Kroeze, J. E.; Hirata, N.; Koops, S.; Nazeeruddin, M. K.; Schmidt-Mende, L.; Grätzel, M.; Durrant, J. R. Alkyl Chain Barriers for Kinetic Optimization in Dye-Sensitized Solar Cells. *J. Am. Chem. Soc.* **2006**, *128*, 16376−16383.